NASA TECHNICAL NOTE

NASA TN D-8299

NASA TN D-8299

DIFFUSION ANALYSIS FOR TWO-PHASE METAL-MATRIX COMPOSITE

Darrel R. Tenney

Langley Research Center
Hampton, Va. 23665

NATIONAL AERONAUTICS AND SPACE ADMINISTRATION • WASHINGTON, D. C. • DECEMBER 1976

Completed 20 May 77 SM

ERRATA

NASA Technical Note D-8299

DIFFUSION ANALYSIS FOR TWO-PHASE METAL-MATRIX COMPOSITE

Darrel R. Tenney
December 1976

Page 11: The equation for D^{α} should read

$$D^{\alpha} = 3.19 \times 10^{-4} \exp(-4.69C) \exp(-3.69 \times 10^{4}/T) \ m^2/sec$$

Issued March 1977

1. Report No.	2. Government Accession No.	3. Recipient's Catalog No.
NASA TN D-8299		

4. Title and Subtitle
DIFFUSION ANALYSIS FOR TWO-PHASE METAL-MATRIX COMPOSITE

5. Report Date
December 1976

6. Performing Organization Code

7. Author(s)
Darrel R. Tenney

8. Performing Organization Report No.
L-10682

9. Performing Organization Name and Address
NASA Langley Research Center
Hampton, VA 23665

10. Work Unit No.
506-16-21-01

11. Contract or Grant No.

12. Sponsoring Agency Name and Address
National Aeronautics and Space Administration
Washington, DC 20546

13. Type of Report and Period Covered
Technical Note

14. Sponsoring Agency Code

15. Supplementary Notes

16. Abstract

Diffusion-controlled filament-matrix interaction in a metal-matrix composite, where the filaments and matrix comprise a two-phase binary alloy system, has been mathematically modeled. The analysis treats the problem of a diffusion-controlled, two-phase moving interface by means of a one-dimensional, variable-grid, finite-difference technique. Concentration dependent diffusion coefficients and equilibrium solubility limits were used, and the change in filament diameter and compositional changes in the matrix were calculated as a function of exposure time at elevated temperatures. With the tungsten-nickel (W-Ni) system as a model composite system, unidirectional composites containing from 0.06 to 0.44 initial filament volume fraction were modeled. Compositional changes in the matrix were calculated by superposition of the contributions from neighboring filaments. Alternate methods for determining compositional changes between first and second nearest neighbor filaments were also considered. The results show the relative importance of filament volume fraction, filament diameter, exposure temperature, and exposure time as they affect the rate and extent of filament-matrix interaction.

17. Key Words (Suggested by Author(s))	18. Distribution Statement
Tungsten-nickel system Filament-matrix interaction High temperature exposure	Unclassified - Unlimited Subject Category 24

19. Security Classif. (of this report)	20. Security Classif. (of this page)	21. No. of Pages	22. Price*
Unclassified	Unclassified	32	$3.75

* For sale by the National Technical Information Service, Springfield, Virginia 22161

DIFFUSION ANALYSIS FOR TWO-PHASE METAL-MATRIX COMPOSITE

Darrel R. Tenney
Langley Research Center

SUMMARY

Diffusion-controlled filament-matrix interaction in a metal-matrix composite, where the filaments and matrix comprise a two-phase alloy system, has been mathematically modeled. The analysis treats the problem of a diffusion-controlled, two-phase moving interface by means of a one-dimensional, variable-grid, finite-difference technique. Concentration dependent diffusion coefficients and equilibrium solubility limits were used, and the change in filament diameter and compositional changes in the matrix were calculated as a function of exposure time at elevated temperatures. With the tungsten-nickel (W-Ni) system as a model composite system, unidirectional composites containing from 0.06 to 0.44 initial filament volume fraction were modeled. Compositional changes in the matrix were calculated by superposition of the contributions from neighboring filaments. Alternate methods for determining compositional changes between first and second nearest neighbor filaments were also considered. The results show the relative importance of filament volume fraction, filament diameter, exposure temperature, and exposure time as they affect the rate and extent of filament-matrix interaction.

INTRODUCTION

Exposure of a metal-matrix composite to elevated temperature may produce compositional and microstructural changes which result in the modification of composite properties. The extent of these changes depends on the severity of the conditions under which the composite was exposed, the nature of the components of the composite, and the type of filament-matrix interfacial reactions which occur. Based on the type of interfacial reactions, metal-matrix composites can be divided into systems where the filaments and matrix are mutually nonreactive and insoluble (class I), mutually nonreactive but soluble (class II), and reactive, resulting in compound formation (class III). (See ref. 1.) Based on the solubility behavior of the filaments and matrix, class II composites (the material of interest for this study) can be subdivided into systems where (a) the filament and matrix exhibit complete solid solubility, (b) filaments and matrix exhibit limited solid solubility with no intermediate phases, and (c) filaments and matrix exhibit limited solid solubility with one or more intermediate phases.

Any attempt to understand the changes in the mechanical properties of these classes of composites resulting from exposure to elevated temperature logically begins with a knowledge of the chemical and microstructural changes which have occurred. Therefore, for given exposure conditions, a method for calculating the extent of interaction between the filaments and the matrix is necessary.

An analytical technique for calculating compositional changes in class II(a) composites has been previously developed (ref. 2). The present study reports the results of research designed to develop a similar analysis for modeling the compositional changes produced by diffusion between the filaments and matrix for a two-phase composite system of class II(b). A finite-difference analysis employing a variable-grid technique (ref. 3) was used to solve the appropriate diffusion equations. The technique was similar to that employed by Tanzilli and Heckel for homogenization studies (refs. 4 and 5). Two different methods were considered for calculating the compositional changes in the matrix region between filaments. The average change in filament volume fraction with exposure time was calculated by treating the composite as a cylindrical volume element of equivalent filament volume fraction. This approach has the advantage of being independent of filament arrangement and avoids the necessity of a costly and difficult two-dimensional solution of the diffusion equations.

The tungsten-nickel (W-Ni) system was examined as a model class II(b) two-phase composite system. Changes in W filament diameter and compositional changes in the Ni matrix were calculated as a function of exposure time. Analytical results illustrating the influence of initial filament volume fraction and initial filament diameter on change of filament volume fraction at 1323 K and 1418 K are presented.

SYMBOLS

C	atomic fraction B
C'	initial composition of β-phase, atomic fraction B
$\bar{C}$	average composition for sample
C_o	initial composition of α-phase, atomic fraction B
C_n^j	finite-difference notation for composition at station n and time j
C^α, C^β	composition in α- and β-phase regions, atomic fraction B
$C_{\alpha\beta}, C_{\beta\alpha}$	composition in α-phase and in β-phase at $\alpha\beta$ interface equal to solubility limits of α- and β-phases, atomic fraction B
D	diffusion coefficient
D_{max}	maximum diffusion coefficient at temperature of interest in α- or β-phases, m^2/s
$\bar{D}_n$	normalized diffusion coefficient determined by dividing the diffusion coefficient corresponding to composition at grid station n by maximum diffusion coefficient in alloy system at temperature of interest

$g_{\alpha\beta}$ solubility limit of α-phase, volume fraction B

$g_{\beta\alpha}$ solubility limit of β-phase, volume fraction B

I grid point at α-β interface

L/2 radial distance from center of filament to outer boundary of matrix phase, m

ℓ initial thickness of β-phase, m

N grid point at outer boundary

R normalized radial distance from center of filament, $\frac{r}{L/2}$

R_n normalized radial distance from center of filament to finite-difference grid point n

r radial distance from center of filament, m

r_f^o initial radius of filament, m

r_f^* radius of filament when equilibrium has been established between filaments and matrix, m

r_n radial distance from center of filament to finite-difference grid point n, where n ranges from 1 at center of filament to N at outer boundary in α-phase, m

T temperature, K

t time, s

V_f^o initial filament volume fraction of composite

V_f^* filament volume fraction of composite when equilibrium has been obtained between filaments and matrix

δ difference between solubility limits of β- and α-phases, atomic fraction B, $C_{\beta\alpha} - C_{\alpha\beta}$

ξ/2 radial distance from center of filament to filament-matrix interface, m

$\xi^+/2, \xi^-/2$ location of αβ interface where positive superscript designates α side of interface and negative superscript designates β side of interface, m

τ normalized time, $\frac{D_{max}t}{(L/2)^2}$

MATHEMATICAL MODEL

The mathematical modeling of filament-matrix interaction for a class II(b) composite was performed for a unidirectional composite consisting of parallel circular filaments embedded in a matrix of differing material. Although this method of analysis will work for any arrangement of filaments, a symmetrical hexagonal arrangement of filaments was assumed for simplicity. Figure 1(a) shows a schematic view of the cross section of such a composite specimen. The type of compositional changes which occur in a single filament and surrounding matrix region as a result of interdiffusion is illustrated in figure 1(b). The concentration of B atoms is plotted as a function of distance along a line passing through the center of the filament and extending to the edge of the matrix region under consideration ($r = L/2$). The discontinuity in concentration at the filament-matrix interface is equal to the difference between the solubility limits of the β- and α-phases ($C_{\beta\alpha} - C_{\alpha\beta}$). During the diffusion process, B atoms move from the filament into the surrounding matrix, and A atoms move from the matrix into the filament. The filament increases or decreases in diameter, depending on whether the flux of atoms from the filament is less than or greater than the flux of atoms from the matrix into the filament.

A general finite-difference technique was developed to calculate the compositional and dimensional changes which occur in an element like the cylindrical volume element consisting of a single filament and concentric matrix shell illustrated in figure 1(b). The initial filament volume fraction in this element is equal to that of the composite if the outer radius of the matrix shell is equal to $r_f^o \Big/ \sqrt{V_f^o}$ where r_f^o is the initial filament radius and V_f^o is the initial filament volume fraction of the composite. The average amount of filament-matrix interaction in the composite is assumed to be equal to the amount of interaction which occurs in this cylindrical volume element. The justification for making this assumption is discussed in a later section. This paper also shows that one-dimensional solutions calculated for different $L/2$ values can be used to determine approximately the compositional variations over the composite cross section.

Diffusion Equations for Two-Phase System

Diffusion in a solid two-phase system can be described by two partial differential equations (Fick's Second Law) and an interface flux balance equation which describes motion of the interface. For cylindrical coordinates, Fick's Second Law is given by

$$\frac{\partial C}{\partial t} = \frac{1}{r}\frac{\partial}{\partial r}\left(rD(C)\frac{\partial C}{\partial r}\right) \tag{1}$$

The interface flux balance equation can be expressed as

$$(C_{\beta\alpha} - C_{\alpha\beta})\frac{d\xi/2}{dt} = D(C_{\alpha\beta})\left(\frac{dC^{\alpha}}{dr}\right)_{r=\xi^{+}/2} - D(C_{\beta\alpha})\left(\frac{dC^{\beta}}{dr}\right)_{r=\xi^{-}/2} \tag{2}$$

where $C_{\beta\alpha}$ and $C_{\alpha\beta}$ are the concentrations at the interface in the β- and α-phases, $\xi/2$ is the position of the interface, and $\left(\frac{dC^{\alpha}}{dr}\right)_{r=\xi^{+}/2}$ and $\left(\frac{dC^{\beta}}{dr}\right)_{r=\xi^{-}/2}$ are the concentration gradients adjacent to the interface in the α- and β-phases, respectively. The initial and boundary conditions to be satisfied are as follows:

Initial conditions:

$$C = C' \qquad (0 \leqq r < \xi/2; \quad t = 0)$$

$$C = C_o \qquad (\xi/2 < r \leqq L/2; \quad t = 0)$$

Boundary conditions:

$$C = C_{\beta\alpha} \qquad (r = \xi^{-}/2; \quad t > 0)$$

$$C = C_{\alpha\beta} \qquad (r = \xi^{+}/2; \quad t > 0)$$

$$\frac{\partial C^{\beta}}{\partial r} = 0 \qquad (r = 0; \quad t \geqq 0)$$

$$\frac{\partial C^{\alpha}}{\partial r} = 0 \qquad (r = L/2; \quad t \geqq 0)$$

where $\xi^{-}/2$ and $\xi^{+}/2$ refer to the β and α sides of the interfaces.

In general, the thicknesses of the α- and β-phases change with diffusion time. To account for these dimensional changes, the variable-grid technique developed by Murray and Landis (ref. 3) was used. The number of stations in each phase was fixed and the grid sizes Δr^{α} and Δr^{β} were changed with time. The definition of these grid spacings, in terms of the grid point notation to be used in the following mathematical development, is illustrated in figure 2. The β-phase was divided into I - 1 equally sized space increments of thickness Δr^{β}. The α-phase was divided into N - I increments of thickness Δr^{α}. With this type of grid arrangement, the location of any internal grid point was always a constant percentage of the instantaneous phase thickness. The rate of travel of any grid point n is related to the velocity of the interface by

$$\frac{dr_n}{dt} = \frac{r_n}{\xi/2} \frac{d(\xi/2)}{dt} \tag{3}$$

The rate of change of concentration at any internal station can be expressed as

$$\frac{dC_n}{dt} = \frac{\partial C_n}{\partial r_n}\left(\frac{dr_n}{dt}\right) + \frac{\partial C_n}{\partial t} \tag{4}$$

where $\frac{\partial C_n}{\partial r_n}\left(\frac{dr_n}{dt}\right)$ is the change in concentration because of motion of the grid station with respect to the end of the diffusion couple, and $\partial C/\partial t$ is the contribution of equation (1) (Fick's Second Law). By combining equations (3) and (4), an expression for the variation of concentration with time at an internal station n in the β-phase can be written as follows:

$$\frac{dC_n^{\beta}}{dt} = \frac{r_n}{\xi/2}\frac{\partial C_n}{\partial r_n}\frac{d(\xi/2)}{dt} + \frac{\partial C_n}{\partial t} \tag{5}$$

In analogous fashion, the change in concentration with time at an internal station n in the α-phase, relative to the stationary α-phase boundary at $r = L/2$, is given by

$$\frac{dC_n^{\alpha}}{dt} = \left(\frac{L/2 - r_n}{L/2 - \xi/2}\right)\frac{\partial C_n}{\partial r_n}\frac{d(\xi/2)}{dt} + \frac{\partial C_n}{\partial t} \tag{6}$$

These equations can be normalized by using the change of variables

$$R = \frac{r}{L/2}$$

$$\tau = \frac{D_{max}t}{(L/2)^2}$$

$$\bar{D}_n = \frac{D(C_n)}{D_{max}}$$

where D_{max} is the maximum diffusion coefficient in the system at the temperature of interest. By using these variables, equations (5) and (6) can be rewritten to give

β-phase:

$$\frac{dC_n^{\beta}}{d\tau} = \frac{R_n}{\xi/L}\frac{\partial C_n}{\partial R_n}\frac{d(\xi/L)}{d\tau} + \frac{\partial C_n}{\partial \tau} \tag{7}$$

α-phase:

$$\frac{dC_n^{\alpha}}{d\tau} = \left(\frac{1 - R_n}{1 - \xi/L}\right)\frac{\partial C_n}{\partial R_n}\frac{d(\xi/L)}{d\tau} + \frac{\partial C_n}{\partial \tau} \tag{8}$$

Substitution of the normalized variables into equations (1) and (2) gives

$$\frac{\partial C_n}{\partial \tau} = \bar{D}_n\left(\frac{1}{R_n}\frac{\partial C}{\partial R_n} + \frac{\partial^2 C_n}{\partial R_n^2}\right) + \frac{\partial \bar{D}_n}{\partial R_n}\frac{\partial C_n}{\partial R_n} \tag{9}$$

and

$$\frac{d(\xi/L)}{d\tau} = \left(\frac{1}{\delta}\right)\left[\bar{D}_{\alpha\beta}\left(\frac{dC^{\alpha}}{dR}\right)_{r=\xi^+/2} - \bar{D}_{\beta\alpha}\left(\frac{dC^{\beta}}{dR}\right)_{r=\xi^-/2}\right] \tag{10}$$

where $\delta = C_{\beta\alpha} - C_{\alpha\beta}$.

Combining equations (7) and (9) and rewriting in finite-difference notation (explicit form, second-order central difference) leads to the following expressions for the β-phase:

$$\frac{C_n^{j+1} - C_n^{j}}{\Delta\tau} = \frac{R_n}{\xi/L}\frac{d(\xi/L)}{d\tau}\frac{C_{n+1}^{j} - C_{n-1}^{j}}{2\,\Delta R} + \frac{\partial C_n^{\beta}}{\partial \tau} \tag{11}$$

where

$$\frac{\partial C_n^{\beta}}{\partial \tau} = \bar{D}_n\left[\frac{1}{R_n}\frac{C_{n+1}^{j} - C_{n-1}^{j}}{2\,\Delta R^{\beta}} + \frac{C_{n+1}^{j} - 2C_n^{j} + C_{n-1}^{j}}{(\Delta R^{\beta})^2}\right] + \frac{\bar{D}_{n+1} - \bar{D}_{n-1}}{2\,\Delta R^{\beta}}\frac{C_{n+1}^{j} - C_{n-1}^{j}}{2\,\Delta R^{\beta}}$$

Combining equations (8) and (9) and similarly rewriting in finite-difference notation gives the following expressions for the α-phase:

$$\frac{C_n^{j+1} - C_n^j}{\Delta\tau} = \left(\frac{1 - R_n}{1 - \xi/L}\right)\frac{C_{n+1}^j - C_{n-1}^j}{2\,\Delta R^\alpha}\,\frac{d(\xi/L)}{d\tau} + \frac{\partial C_n^\alpha}{\partial\tau} \tag{12}$$

where

$$\frac{\partial C_n^\alpha}{\partial\tau} = \bar{D}_n\left[\frac{1}{R_n}\,\frac{C_{n+1}^j - C_{n-1}^j}{2\,\Delta R^\alpha} + \frac{C_{n+1}^j - 2C_n^j + C_{n-1}^j}{(\Delta R^\alpha)^2}\right] + \frac{\bar{D}_{n+1} - \bar{D}_{n-1}}{2\,\Delta R^\alpha}\,\frac{C_{n+1}^j - C_{n-1}^j}{2\,\Delta R^\alpha}$$

The finite-difference expression (second-order forward and reverse difference) for the interface mass balance equation (eq. (10)) is given by

$$\frac{d(\xi/L)}{dt} = \left(\frac{1}{\delta}\right)\left(\bar{D}_{\alpha\beta}\,\frac{-C_{I+2}^j + 4C_{I+1}^j - 3C_{\alpha\beta}^j}{2\,\Delta R^\alpha} - \bar{D}_{\beta\alpha}\,\frac{C_{I-2}^j - 4C_{I-1}^j + 3C_{\beta\alpha}^j}{2\,\Delta R^\beta}\right) \tag{13}$$

At grid point $n = 1$, corresponding to the center of the β filament, the finite-difference expression of equation (7) reduces to

$$\frac{C_1^{j+1} - C_1^j}{\Delta\tau} = 4\bar{D}_1\left[\frac{C_2^j - C_1^j}{(\Delta R^\beta)^2}\right] \tag{14}$$

To obtain this expression, a second-order forward difference was used and the singularity in the differential equation (eq. (9)) at $R = 0$ was taken into account (ref. 6).

In analogous fashion, equation (8) at station $n = N$, corresponding to the outer boundary at $R = 1$ ($r_N = L/2$) (see fig. 2), reduces to

$$\frac{C_N^{j+1} - C_N^j}{\Delta\tau} = 2\bar{D}_N\left[\frac{C_{N-1}^j - C_N^j}{(\Delta R^\alpha)^2}\right] \tag{15}$$

To perform the finite-difference calculations, the grid spacings must be small enough to give convergent solutions of acceptable accuracy. Since explicit formulation was used in the development of these equations, the time increment $\Delta\tau$ was selected according to the stability requirement that $\Delta\tau \leq \frac{1}{4}(\Delta R^2)$. The procedure employed was to calculate $\Delta\tau$ using either ΔR^α or ΔR^β, whichever was smaller. For each solution, a check for conservation of mass was performed.

If there was a deviation of 2 percent or greater in conservation, the number of grid points in each phase was increased and the solution was recalculated.

As an additional check on solution accuracy, a typical test case was considered for which the grid sizes in the filament and matrix were varied in an effort to establish the optimum grid size for which a convergent solution of acceptable accuracy could be obtained. An accurate solution was defined as one for which the shift of the filament-matrix interface, at a given time, showed less than a 2-percent variation as the grid size approached zero ($\Delta r \to 0$). The grid size for all calculations was always taken to be equal to or smaller than the optimum size found for this test case.

Comparison With Experimental Data and Other Methods of Analysis

Although this study is concerned only with cylindrical geometry, the program developed to perform the finite-difference calculations was written to work for planar, cylindrical, or spherical geometries. The program was generalized to all geometries so that a comparison could be made with other analyses available in the literature which work for planar geometry only. Such a comparison was made with results calculated by a closed-form iterative solution technique, reported by Unnam (ref. 7). Comparable solutions were obtained for a wide range of input parameters for planar interfaces (Unnam's solution is valid only for planar interfaces). Different phase thicknesses and assumed changes in diffusion coefficient with composition in each phase were considered to yield information regarding solution stability and accuracy. No significant differences were found between the results obtained from the two different solutions. The interface positions calculated by the finite-difference program were always within 5 percent of the positions calculated by the iterative solution.

Calculations using the analysis of this study were also compared with experimentally determined interdiffusion data on W-Ni laminates, as reported by Tanzilli and Heckel (ref. 8). Tanzilli and Heckel prepared multilayer W-Ni couples by diffusion bonding alternate layers of pure Ni and pure W. Samples were made with two overall mean compositions, $\bar{C} = 0.152$, and $\bar{C} = 0.121$ atomic fraction W. These W-Ni couples were exposed at 1480 K, after which they were sectioned perpendicular to the layers and were metallographically polished. The extent of interdiffusion was determined by measuring the average thickness of the W- and Ni-rich layers after each exposure, and by electron microprobe analysis of the polished cross sections. The results reported by Tanzilli and Heckel are presented in figure 3, where the normalized thickness of the β-layer ξ/ℓ is plotted as a function of dimensionless time $D^{\alpha}t/\ell^2$. In figure 3, ξ is the β-phase (W-rich) thickness at time t, ℓ is the initial thickness of this layer, and D^{α} is the concentration-independent diffusion coefficient in the α-phase (Ni-rich). Also plotted on this graph are theoretical curves obtained from: (1) a constant-D finite-difference solution developed by Tanzilli and Heckel (ref. 8); (2) the present variable-D finite-difference analysis run with the planar geometry option; and (3) an iterative solution developed by Unnam (ref. 7). The same initial and boundary conditions were used in all three solutions. Theoretical curves are plotted only for the $\bar{C} = 0.152$ sample as there was no difference between the curves for $\bar{C} = 0.152$ or 0.121 until ξ/ℓ dropped below about 0.3. Also, no experimental data points were available below

$\xi/\ell = 0.3$ for the $\bar{C} = 0.121$ sample. The interface positions calculated by all three solutions were in general agreement, but the curve obtained from the variable-D finite-difference analysis used in this study gave the best fit to the experimental data points.

RESULTS AND DISCUSSIONS

The W-Ni phase diagram reported by Hansen (ref. 9) showed only two phases for the temperature range 1273 K to 1873 K. Therefore, this system was selected as a model two-phase class II(b) system. Diffusion calculations were carried out for exposure at 1323 K and 1418 K. The solubility limits in the W-rich and Ni-rich phases at these two temperatures are given in the following table (from ref. 9):

	Solubility limit of -					
	Atomic fraction W at -		Weight fraction W at -		Volume fraction W at -	
	1323 K	1418 K	1323 K	1418 K	1323 K	1418 K
W-phase, $C_{\beta\alpha}$	0.991	0.991	0.997	0.997	0.993	0.993
Ni-phase, $C_{\alpha\beta}$	.166	.168	.385	.388	.214	.216

Tanzilli and Heckel (ref. 8) have experimentally verified (with planar couples) that for W-Ni diffusion couples, interface migration is diffusion controlled, and the interface composition closely approximates the equilibrium compositions which are obtained from the W-Ni phase diagram (ref. 9).

In the computer program developed for this analysis, the concentration was expressed in terms of volume fraction for the computations and was converted back to atomic fraction once the desired solution had been obtained. This conversion was necessary to account for volume changes which occur during diffusion because of differences in the molal volumes of pure W and Ni. Guy, DeHoff, and Smith (ref. 10) have shown that if ideal solution behavior is assumed, the concentration can be defined in terms of volume fraction without altering the form of Fick's laws. To check the validity of assuming ideal solution behavior for the Ni-rich region of the W-Ni system, a plot of the molal volume of the solid solution was made as a function of composition. A nearly linear relationship indicating approximately ideal solution behavior existed between these two quantities.

The interdiffusion coefficient data of Walsh and Donachie (ref. 11) were used for the alpha solid solution of W in Ni. Walsh and Donachie reported that the concentration dependence of D in the temperature range 1273 K to 1589 K could be represented by

$$D^{\alpha} = 3.19 \times 10^{-4} \exp(-4.69C) \exp(-3.69 \times 10^4/T)\ m^2/sec$$

where C is the W concentration in atomic fraction. (There is a discrepancy in the report of Walsh and Donachie. The constant term in the equation just given was reported as 1.19 instead of the correct value of 3.19.) For the W-rich β-phase, the W self-diffusion data of Vasilev and Chernomorchenko (ref. 12) were used:

$$D_0 = 6.3 \times 10^3\ m^2/sec$$

$$Q = 135.8\ kcal/mol$$

These concentration-dependent diffusion coefficients and the tabulated equilibrium solubility limits were used in the finite-difference analysis previously discussed to model interdiffusion in the W-Ni system.

Composition Profiles

Single filament profiles.- Typical concentration profiles for diffusion between a 50-μm-radius W filament and surrounding Ni matrix at 1418 K are shown in figure 4. The atomic fraction of W is plotted as a function of distance in micrometers from the center of the W filament. Curves for exposure times of 10, 100, 200, and 500 hours are shown. The W-Ni interface moves into the W filament with increasing exposure time because the flux of W atoms from the filament into the surrounding matrix is larger than the opposite flux of Ni atoms into the filament. There is a difference in mass flow because the rate of diffusion in the Ni-rich phase is approximately two orders of magnitude higher than that in the W-rich phase; the solubility of W in Ni is 0.168 (atomic fraction), whereas the solubility of Ni in W is only 0.009 (atomic fraction).

Composite profiles.- Figure 5 illustrates the composite cross section. The filaments are hexagonally arranged on a cross section perpendicular to the long axes of the filaments. Compositional changes in the composite caused by interdiffusion at elevated temperatures can be characterized by calculating changes which occur within a symmetry cell like the one illustrated in the lower part of figure 5. The symmetry cell shown was selected because it was the simplest cell containing both first and second nearest neighbor filaments.

The radial solution calculated by the finite-difference analysis presented earlier was used to determine approximately the composition at any point in the composite cross section. This was accomplished by superposition of the contributions from neighboring filaments. A three-dimensional view of the tungsten compositional variation over the cross section of a 0.40 volume fraction W filament-Ni matrix composite, calculated by superposition, is shown in figure 6. The composite contained 0.40 volume fraction W filament and was exposed

for 100 hours at 1418 K. The atomic fraction W is plotted on the vertical axis with distance in micrometers plotted along the horizontal axis. The left front face of the element shows a cross section through the centers of second nearest neighbor filaments (E and C in fig. 5). The right front face shows a similar cross section through the centers of first nearest neighbor filaments (C and B in fig. 5). The profile between centers of first nearest neighbor filaments shows a simple "U-shape" with a minimum midway between the filaments. The profile between centers of second nearest neighbors has a small relative maximum in the center with minima on each side. The concentration maximum is caused by diffusion from the two first nearest neighbor filaments located on either side of the maximum.

First nearest neighbor profiles.- Figure 5 illustrates the symmetry element. Filaments A and C are first nearest neighbor filaments. If the midpoint of the line connecting the centers of these filaments is assumed to be a zero flux location, the composition profile from the center of filament A to the midpoint Q can be directly calculated by the finite-difference technique presented earlier. This calculation is accomplished by letting L/2 equal AQ, where L/2 is the location in the α-phase Ni matrix, and where the zero flux boundary condition is imposed. (See fig. 2.) The other half of the nearest neighbor profile, from Q to C, is obtained by taking the mirror image of the profile from A to Q. This method of profile calculation is referred to as symmetry point analysis.

Figure 7 shows a comparison of first nearest neighbor profiles calculated by symmetry point analysis and by superposition. The atomic fraction W is plotted as a function of distance between centers of nearest neighbor filaments for composites which initially contained 0.23 and 0.40 volume fraction W filaments. The exposure conditions were 500 hours at 1418 K. In both composites, the initial radius of the W filaments was 50 μm.

Profiles calculated by superposition and by symmetry point analysis were nearly identical for diffusion times up to 500 hours for the 0.23 volume fraction composite. Good agreement between the results of the two methods was also observed for the 0.40 volume fraction composite for short times when the extent of interdiffusion was low. However, the 500-hour exposure condition resulted in a significant difference between the two profiles. The symmetry point profile indicates that the Ni matrix was saturated at the theoretical solubility limit for 1418 K. The superposition profile exceeded this limit over nearly half the matrix region, the largest difference occurring near the filaments. Since the solubility limit of the matrix phase is exceeded, the amount of interface motion must be too large. Both of these errors arise because superposition does not consider any filament-filament interaction. Symmetry point analysis, however, does take interaction into account and should be used for cases where the matrix approaches saturation. Superposition was accurate for exposure conditions with low to moderate degrees of interaction but was subject to inaccuracy for conditions where substantial profile interaction occurred.

Second nearest neighbor profiles.- If the filaments are hexagonally arranged, the second nearest neighbor filaments are those located at the ends of the long diagonal of the symmetry cell shown in figure 5. The simplest way to calculate compositional changes along the diagonal line connecting second

nearest neighbor filaments is to superimpose the contributions of the filaments located at the corners of the symmetry element. These four filaments are the primary contributors, and the presence of other filaments located further from the body diagonal line was neglected because their contributions were expected to be small.

Concentration profiles between second nearest neighbor filaments, calculated by superposition for a 0.40 volume fraction composite, are shown in figure 8. Curves for exposure times of 10, 100, 200, and 500 hours at 1418 K are presented. With increasing exposure time, the W filament diameter decreases and the concentration of W in the Ni matrix increases. The 100- and 200-hour compositional profiles show a small central maximum in the Ni matrix, midway between the second nearest neighbor filaments. As noted earlier, this maximum is clearly caused by the contribution of filaments A and C located adjacent to the center section in figure 5. The 500-hour composition profile exceeds the solubility limit of W in Ni in the Ni matrix adjacent to the filaments. The interaction is too large for accurate results to be obtained by superposition.

By using the symmetry found along the body diagonal line to define boundary conditions, an alternate method for determining the compositional profiles between second nearest neighbors can be performed. Definition of the boundary conditions permits a direct finite-difference calculation of the compositional changes over the end sections near the filaments. The remainder of the profile, over the center section, must then be calculated by superposition or it must be estimated. The rationale for this approach can best be understood by again referring to the hexagonal symmetry element shown in figure 5. Points P and R, located at the centers of equilateral triangles ACD and ABC, are zero flux locations. By setting L/2 = DP and by using the symmetry point analysis, the concentration profile from the centers of the filaments on each end, B and D, to the minima points, P and R, can be calculated. The composition at the center, point Q, can be obtained from the profile (calculated by symmetry point analysis) between first nearest neighbor filaments A and C. Point Q has the maximum composition found over the central portion of the profile along the body diagonal. When the values of the composition at each of the three extremum points along line BD are known, the approximate shape of the composition contour over the central region can be estimated by curve fitting.

Concentration profiles between second nearest neighbor filaments for a 0.40 volume fraction W-Ni composite exposed at 1418 K for times of 10, 100, 200, and 500 hours are shown in figure 9. The parts of the profiles shown by solid lines were calculated by symmetry point analysis. The central portions shown with dashed lines were estimated. The circled center point was obtained from first nearest neighbor profile solutions calculated for a 0.40 volume fraction composite exposed to the same temperature and time. The calculated profiles adjacent to the fiber, generally the regions of greatest interest, should be reasonably accurate even for large degrees of interaction. The same is true for the central maximum point. Thus, although the remainder of the profile had to be estimated, this general approach should give reasonably accurate profiles even for cases of extensive interaction.

The 200 hour, 1418 K exposure profiles calculated by superposition and symmetry point analysis, shown previously in figures 8 and 9, are compared in

figure 10. The symmetry point profile is lower than the superposition profile in the Ni matrix regions adjacent to the W filaments but rises slightly above the superposition profile in the central region. The superposition profile is clearly too high in the matrix region adjoining the filament since it predicts an interface composition higher than the theoretical solubility limit of W in Ni. For times shorter than 200 hours at 1418 K, the profiles calculated by the two techniques were nearly identical. However, for longer times, inaccuracies in the superposition technique result in a progressively larger difference between the curves calculated by the two methods.

Initial Filament Volume Fraction Effects

If a composite is exposed until equilibrium is established between the filaments and matrix, the equilibrium filament volume fraction V_f^* can be related to the initial filament volume fraction V_f^o by

$$V_f^* = \frac{V_f^o - g_{\alpha\beta}}{g_{\beta\alpha} - g_{\alpha\beta}}$$

where $g_{\beta\alpha}$ and $g_{\alpha\beta}$ are the solubility limits of the filament and matrix phases expressed in terms of volume fraction B atoms. For a unidirectional composite containing cylindrical filaments, the ratio of the equilibrium filament radius r_f^* to the initial filament radius r_f^o is given by

$$\frac{r_f^*}{r_f^o} = \sqrt{\frac{1 - g_{\alpha\beta}/V_f^o}{g_{\beta\alpha} - g_{\alpha\beta}}}$$

This relationship shows that if the initial filament volume fraction is less than the solubility limit of the matrix phase $g_{\alpha\beta}$, the filaments disappear before equilibrium is reached. This relationship also shows that $g_{\alpha\beta}$ is a dominant material parameter for the composite in that the smaller $g_{\alpha\beta}$ is, the smaller the net reduction in filament diameter at equilibrium.

Typical change in concentration profiles.- Concentration profiles between centers of the first nearest neighbor filaments for two composites containing initially different filament volume fractions are shown in figure 11. The exposure conditions were 1418 K for times of 10, 100, 200, and 500 hours. Symmetry point analysis was used to calculate the resulting diffusion profiles for composites which contained initial filament volume fractions of approximately 0.23 and 0.40. The effect of filament volume fraction on the distance that the filament-matrix interface moved with exposure time is evident. Since the filament spacing in the 0.40 volume fraction composite is smaller than in the

0.23 volume fraction composite, the Ni matrix between filaments saturates in a shorter time.

Although V_f^o determines how much each filament is reduced in diameter at equilibrium, the rate at which a composite proceeds toward equilibrium saturation is primarily determined by the exposure temperature. Figure 12 shows a comparison of calculated nearest neighbor composition profiles for a 0.40 volume fraction composite exposed at 1418 K and 1323 K for 200 hours. Because diffusion is exponentially dependent on temperature, a change of only 95 K was sufficient to cause the W-Ni interface to move more than twice as far at 1418 K as at 1323 K.

Average change in filament volume fraction.- To calculate the average filament volume fraction decrease in a unidirectional composite with exposure time, the composite was treated as a cylindrical volume element having the same initial filament volume fraction V_f^o as that of the composite. This element consists of a filament surrounded by a concentric matrix shell with an outer diameter of $r_f^o/\sqrt{V_f^o}$ where r_f^o is the initial filament radius, and V_f^o is the initial filament volume fraction of the composite.

A typical volume fraction decrease curve calculated for a W-Ni composite exposed at 1418 K is shown in figure 13. Also shown are curves calculated by letting the location of the outer boundary L/2 (see fig. 1) be equal to distances AP and AQ defined in the composite symmetry element shown in figure 5. The distance $L/2 = r_f^o/\sqrt{V_f^o}$ is larger than AQ but less than AP. The curves calculated for L/2 = AQ and AP form upper and lower bounds on the true volume fraction decrease curve. The composite symmetry element in the upper left of figure 13 shows that matrix cylinders of radius AQ concentric about each filament do not contain the entire matrix. Because the shaded area between filaments is not included, the volume fraction decrease curve determined for L/2 = AQ levels off above the true equilibrium value. Matrix cylinders of radius AP, concentric about each filament, overlap and consequently contain more than the available matrix volume. Therefore, the volume fraction decrease curve for L/2 = AP reaches equilibrium below the true equilibrium. If a two-dimensional analysis of diffusion in the composite were carried out, the volume fraction decrease curve calculated would be the $L/2 = r_f^o/\sqrt{V_f^o}$ curve in the initial stages and would go to the same limiting value. This behavior follows because in the initial stage, only radial diffusion from the filaments occurs, and the limiting value is determined only by equilibrium solubility conditions.

Plotting the movement of the filament-matrix interface and corresponding change in filament volume fraction as a function of exposure time at different temperatures clarifies the combined effects of temperature and V_f^o on filament-matrix interaction. Such plots for exposure at 1323 K and 1418 K are presented in figure 14. Curves are presented for composites containing initial filament

volume fractions of 0.06, 0.25, and 0.44. At 1323 K, essentially the same interface shift and changes in filament volume fraction were found for composites containing from 0.06 to 0.44 initial filament volume fractions. This similarity indicates that, for these cases, the concentration in the matrix was not large enough to affect the amount of diffusion. This condition was not, however, true for the 1418 K exposure condition. For exposure times longer than 200 hours, the movement of the filament-matrix interface was dependent on the filament volume fraction. Concentration buildup in the matrix slows the diffusion process sooner for high filament volume fraction composites than for low filament volume fraction composites.

Initial Filament Diameter Effects

Initial filament diameter as well as initial filament volume fraction and exposure temperature affect the change in filament volume fraction with exposure time. Curves in figure 15 show the change in filament volume fraction with exposure time for composites initially containing 0.44 and 0.25 volume fraction filaments. Results are presented for initial filament diameters of 20, 40, 60, 100, and 160 μm. The smaller the diameter, the larger the number of filaments per unit cross-sectional area for a given volume fraction. The curves show that the smaller the filament diameter, the faster the reduction in filament volume fraction with exposure time. The primary reason for this behavior is that during the early stages of interdiffusion, the filament-matrix interface moves approximately the same distance independent of filament diameter. However, a given interface shift produces a much larger percentage of decrease in filament volume fraction for a composite with small diameter filaments than for a composite with larger diameter filaments. The equilibrium filament volume fraction does not depend on filament size; rather, it depends only on the initial filament volume fraction of the composite and the solubility limits of the filament and matrix. The limiting volume fraction is reached first for a high volume fraction composite containing small filaments.

CONCLUDING REMARKS

Interdiffusion between filaments and matrix in a two-phase metal-matrix composite system with limited solid solubility and no intermediate phases was analyzed. The tungsten-nickel (W-Ni) system (W filaments, Ni matrix) was used as a model two-phase composite system. Compositional changes and decrease in filament volume fraction with exposure time at 1323 K and 1418 K were calculated for composites containing initially different filament volume fractions and filaments of different diameters. Two different methods, superposition and symmetry point analysis, were used to calculate compositional changes between first and second nearest neighbor filaments. Both methods gave essentially the same results for short exposure times or low degrees of filament-filament interaction. However, for exposure conditions which resulted in high degrees of interaction, superposition predicted too great a shift of the tungsten-nickel interface and concentrations in the matrix in excess of the theoretical solubility limit for tungsten in nickel. These errors occurred because superposition did not take

into account any filament-filament interaction. Symmetry point analysis, however, did account for interaction and gave a more accurate estimate of composition variation between filaments and the distance the interface moved.

Calculations were performed to determine the average change in filament volume fraction with exposure time for composites containing initially different filament volume fractions and filament diameters. For these calculations, each composite was treated as a cylindrical volume element having the same initial filament volume fraction as that of the composite. Results for tungsten-nickel (W-Ni) composites exposed at 1323 K and 1418 K showed that temperature was more important in controlling the rates of decrease of filament volume fraction with exposure time than either the differences in initial filament volume fraction or differences in initial filament diameter. The initial filament volume fraction affected the rate of interaction only for exposure times long enough to give rise to significant filament-filament interaction. The initial filament diameter, however, had a strong effect on the initial rate of decrease of filament volume fraction but became less important as homogenization proceeded. The relative importance of each of these variables can be calculated for any two-phase binary alloy composite by the analysis developed in this paper.

Langley Research Center
National Aeronautics and Space Administration
Hampton, VA 23665
October 5, 1976

REFERENCES

1. Metcalfe, Arthur G., ed.: Interfaces in Metal Matrix Composites. Academic Press, Inc., c.1974.

2. Herring, Harvey W.; and Tenney, Darrel R.: Diffusion in a Unidirectional Filament Reinforced Metal Composite. Metall. Trans., vol. 4, no. 2, Feb. 1973, pp. 437-441.

3. Murray, William D.; and Landis, Fred: Numerical and Machine Solutions of Transient Heat-Conduction Problems Involving Melting or Freezing. Part I - Method of Analysis and Sample Solutions. Trans. ASME, Ser. C: J. Heat Transfer, vol. 81, no. 2, May 1959, pp. 106-112.

4. Tanzilli, R. A.; and Heckel, R. W.: Numerical Solutions to the Finite, Diffusion-Controlled, Two-Phase, Moving-Interface Problem (With Planar, Cylindrical, and Spherical Interfaces). Trans. Met. Soc. AIME, vol. 242, no. 11, Nov. 1968, pp. 2313-2321.

5. Tanzilli, R. A.; and Heckel, R. W.: A Normalized Treatment of the Solution of Second Phase Particles. Trans. Met. Soc. AIME, vol. 245, no. 6, June 1969, pp. 1363-1366.

6. Crank, J.: The Mathematics of Diffusion. Oxford Univ. Press, 1956.

7. Unnam, Jalaiah: X-Ray Diffraction Technique for the Study of Bi-Metallic, Two-Phase, Diffusion Zones, With Application to Copper-Silver Alloy System. Ph. D. Thesis, Virginia Polytech. Inst. and State Univ., 1976.

8. Tanzilli, R. A.; and Heckel, R. W.: An Analysis of Interdiffusion in Finite-Geometry, Two-Phase Diffusion Couples in the Ni-W and Ag-Cu Systems. Metall. Trans., vol. 2, no. 7, July 1971, pp. 1779-1784.

9. Hansen, Max: Constitution of Binary Alloys. Second ed. McGraw-Hill Book Co., Inc., 1958.

10. Guy, A. G.; DeHoff, R. T.; and Smith, C. B.: Calculation of Interdiffusion Coefficients Considering Variations in Atomic Volume. Trans. American Soc. Met., vol. LXI, no. 2, June 1968, pp. 314-320.

11. Walsh, J. M.; and Donachie, M. J., Jr.: Interdiffusion in the Nickel-Tungsten and Thoria-Dispersed Nickel-Tungsten Systems. Met. Sci. J., vol. 3, Mar. 1969, pp. 68-74.

12. Vasilev, V. P.; and Chernomorchenko, S. G. (Helen J. Chick and Richard Bidwell, trans.): On a Method of Study of the Self-Diffusion of Tungsten. AEC-tr-4276, Los Alamos Sci. Lab., Univ. of California, [1956].

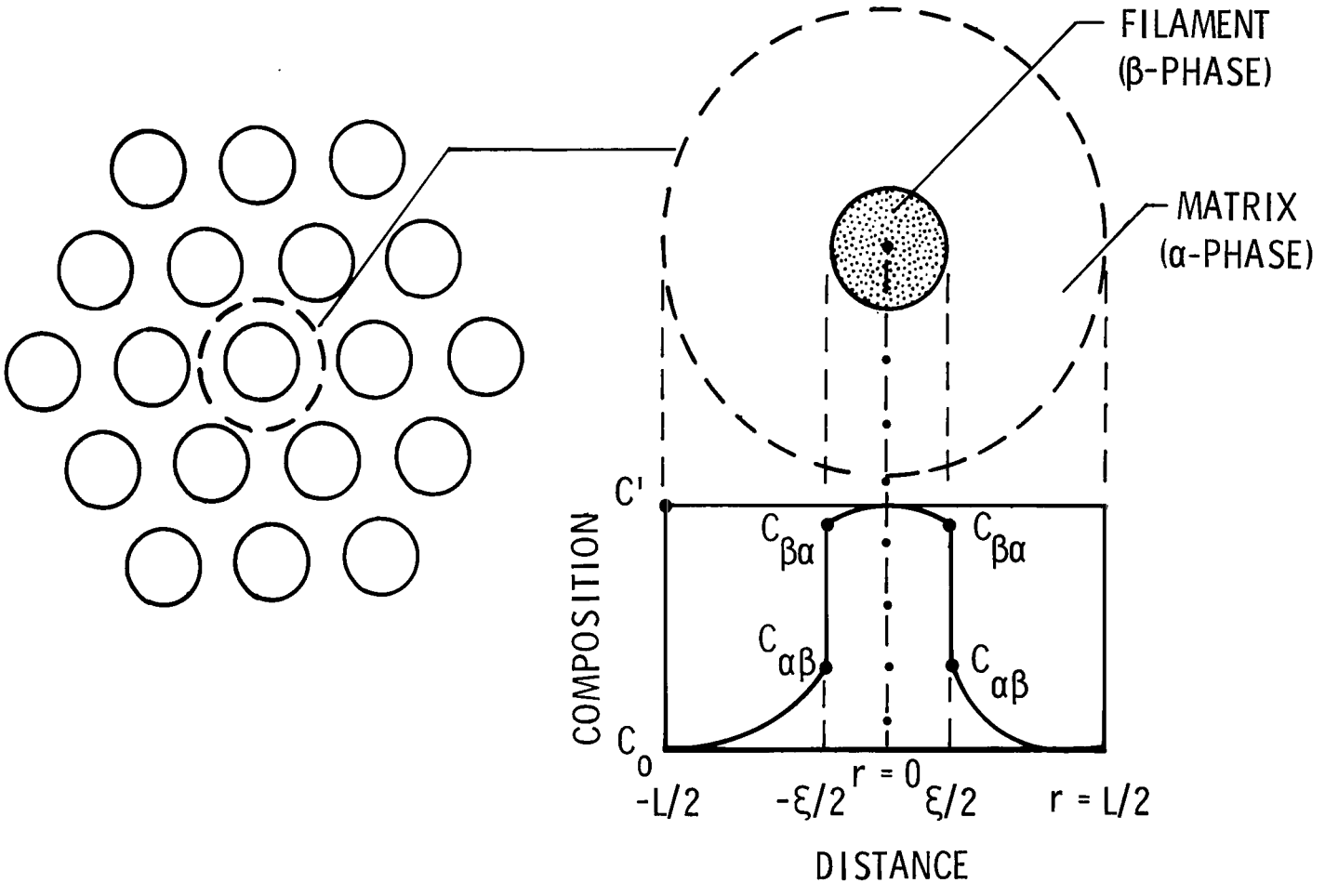

(a) Cross section of unidirectional composite.

(b) Equivalent composite volume element.

Figure 1.- Composition variation due to diffusion between filament and matrix.

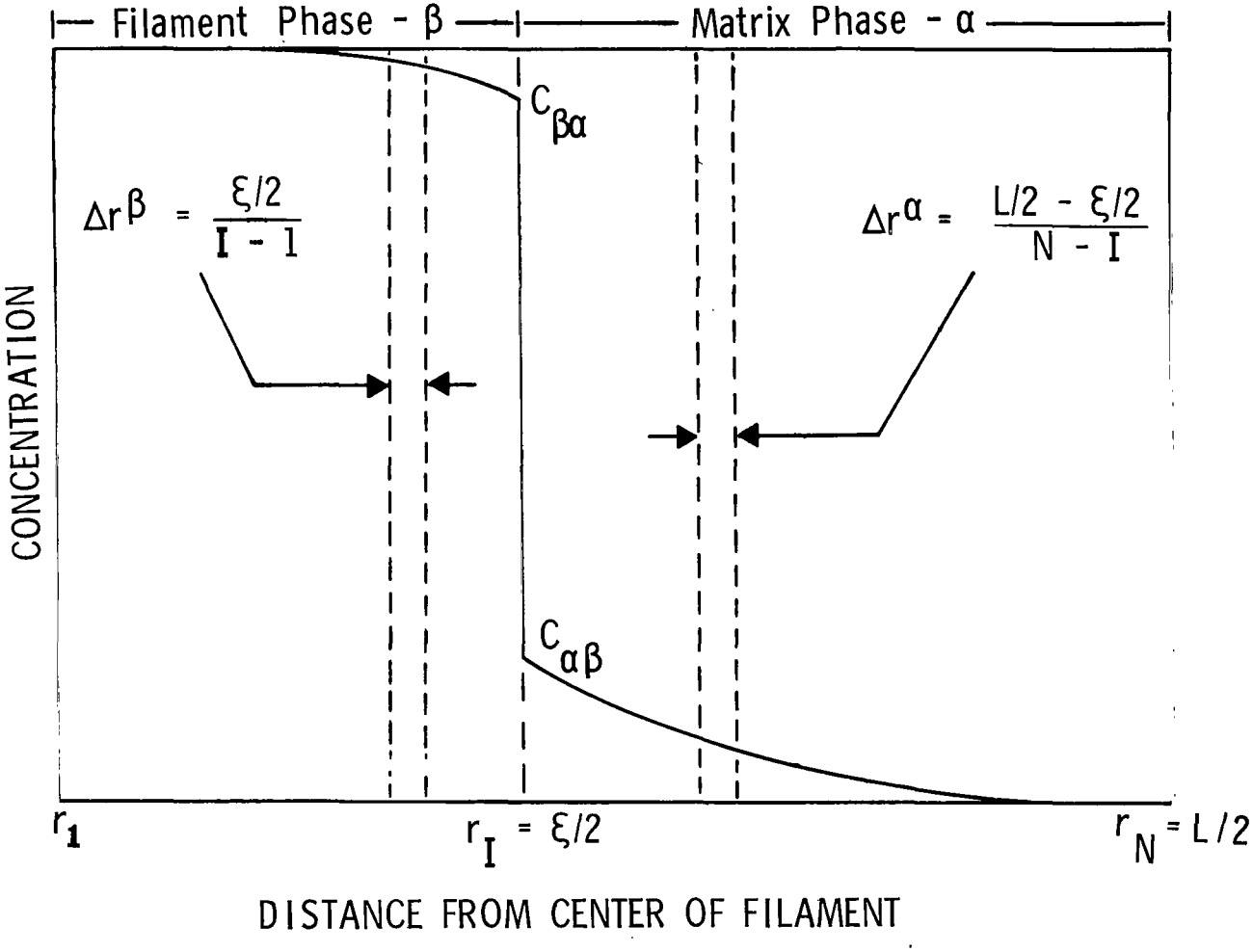

Figure 2.- Schematic cross section of diffused two-phase composite showing filament-matrix interface and definition of parameters used in finite-difference analysis.

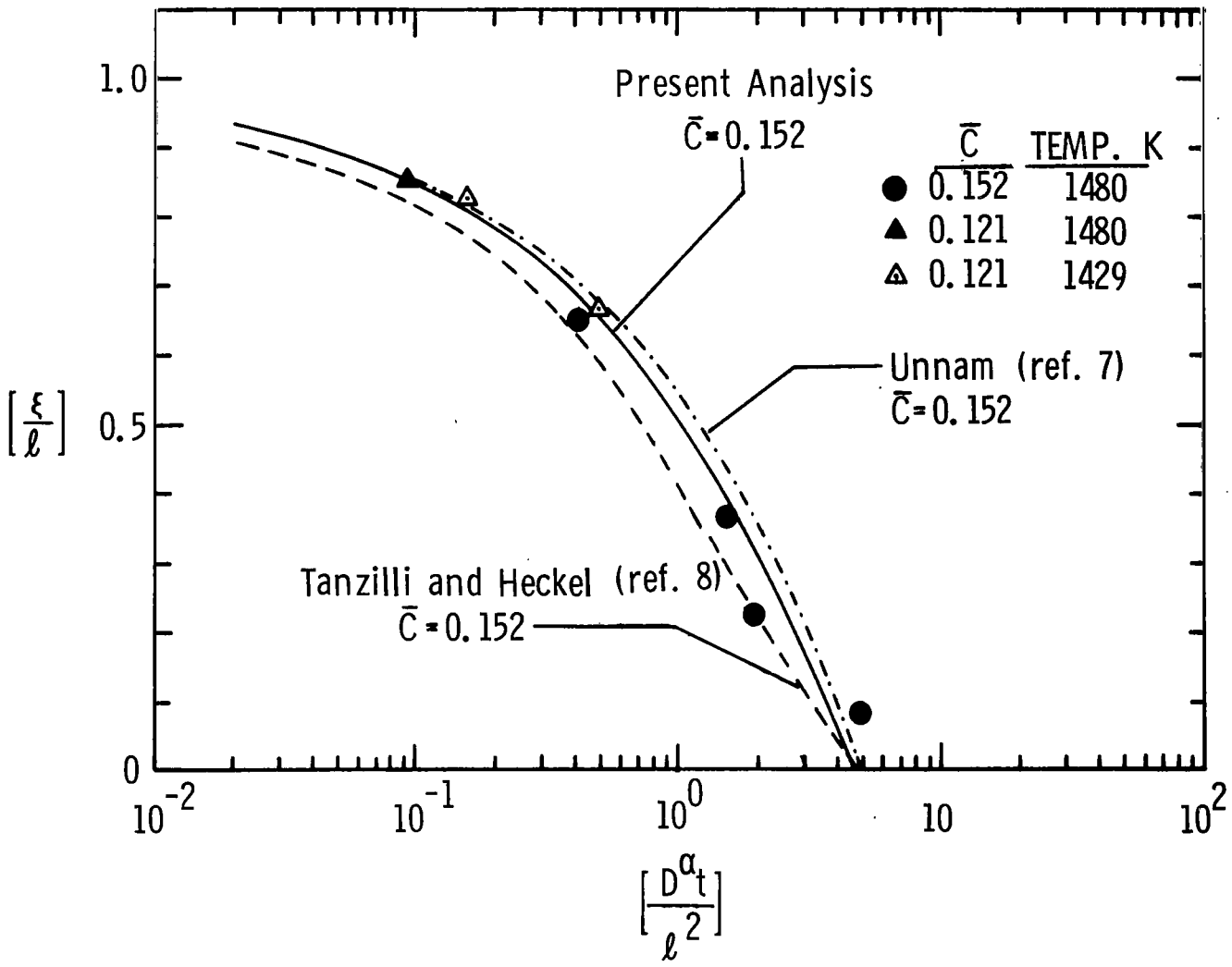

Figure 3.- Comparison of calculated and experimental interface migration data for planar W-Ni couples.

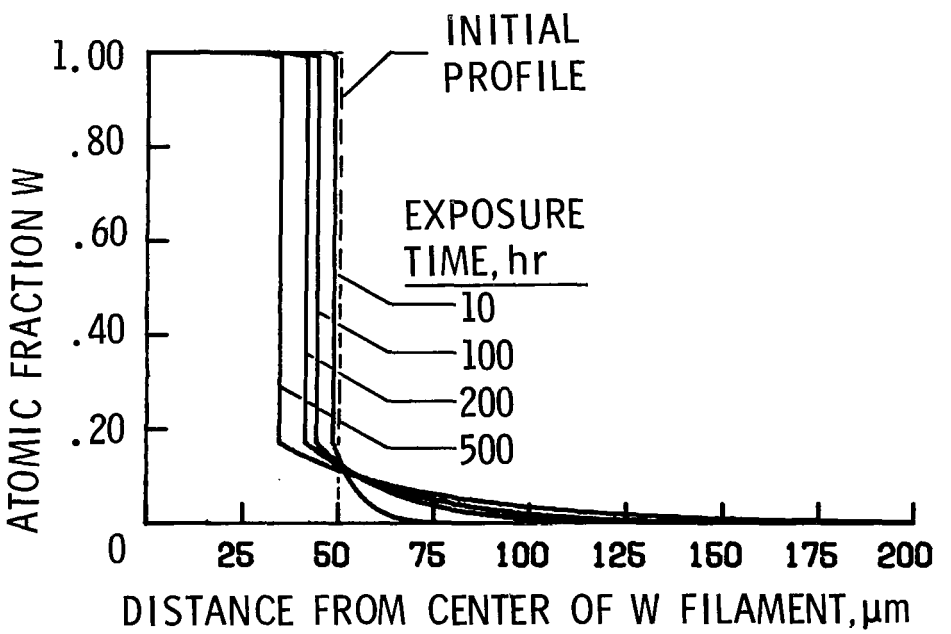

Figure 4.- Concentration profiles for single W filament embedded in Ni matrix and exposed at 1418 K.

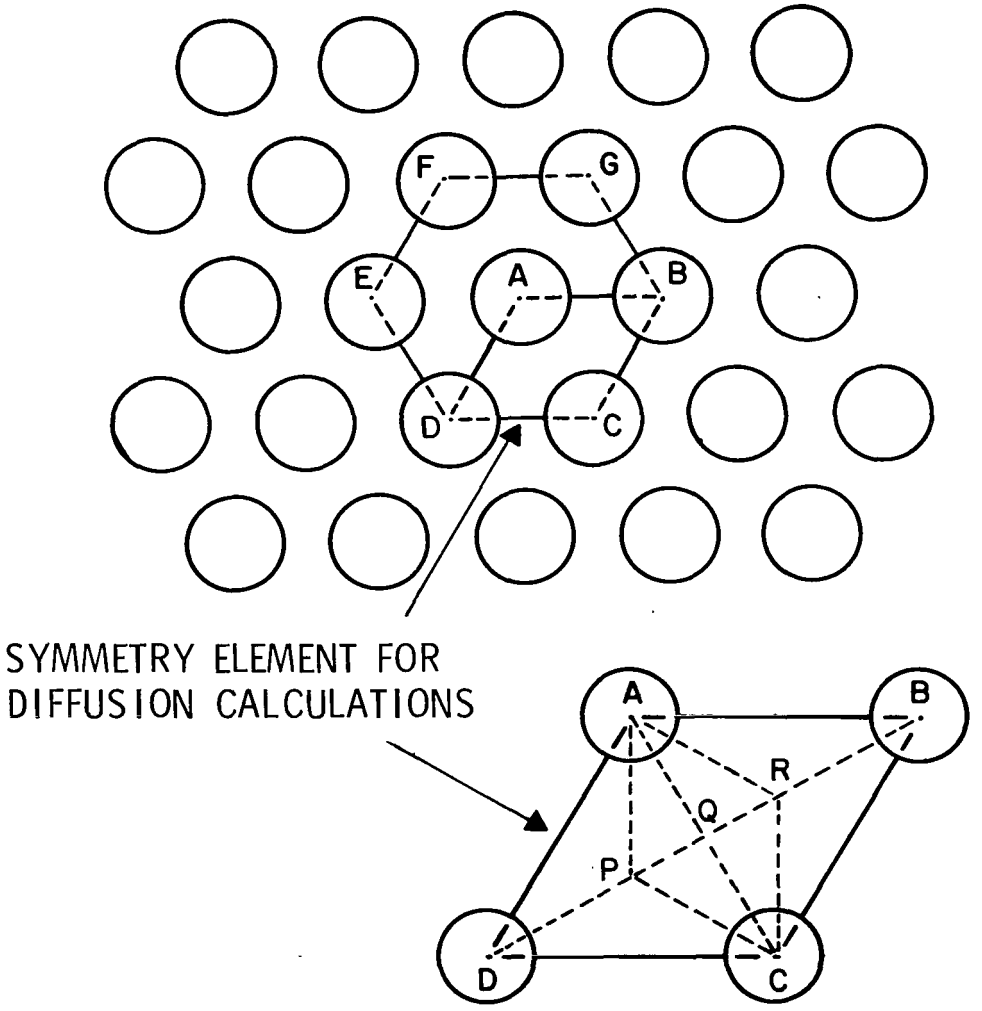

Figure 5.- Idealized arrangement of filaments in metal-matrix composite.

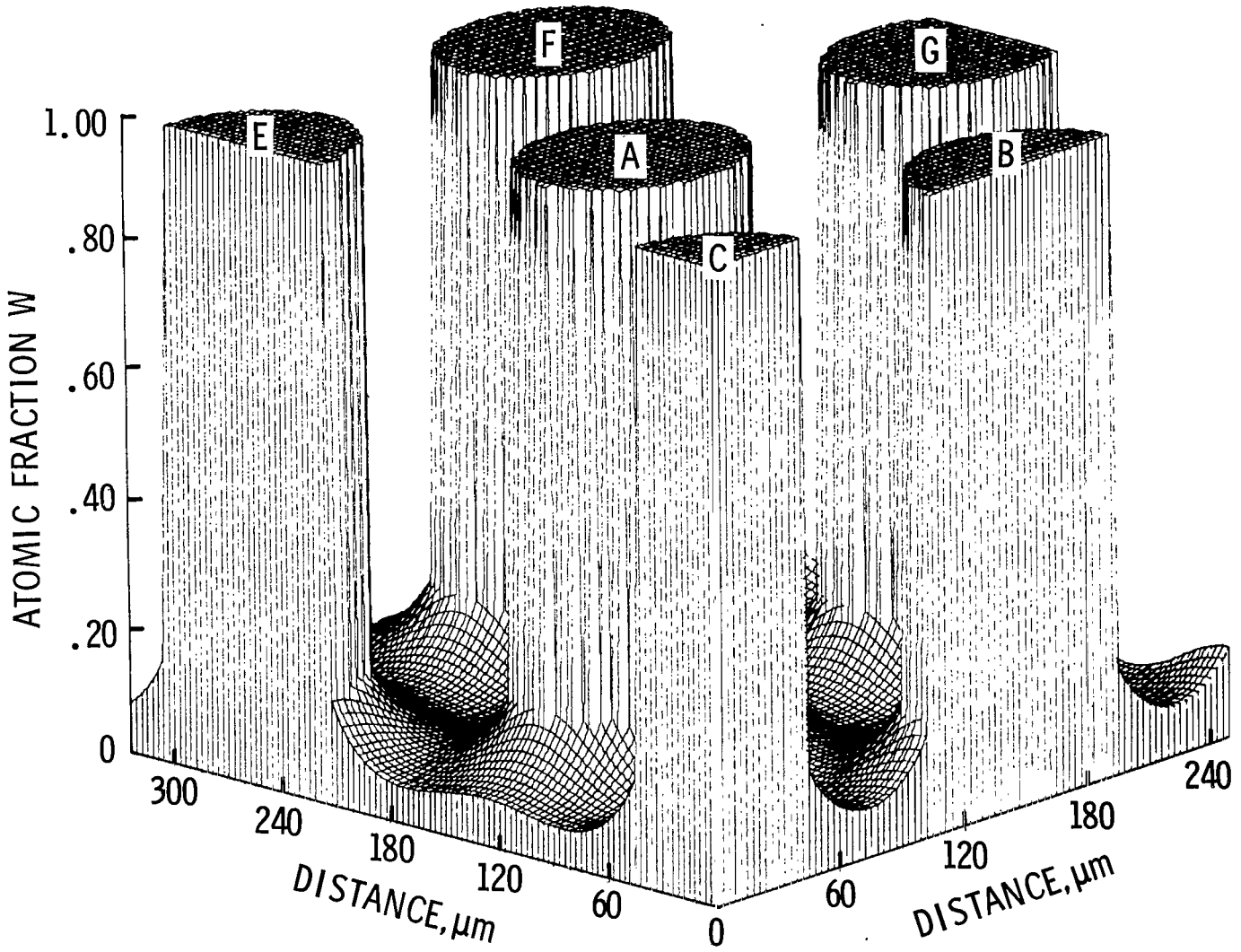

Figure 6.- Three-dimensional perspective view of W composition variation over cross section of 0.40 volume fraction W-Ni composite exposed at 1418 K for 100 hours.

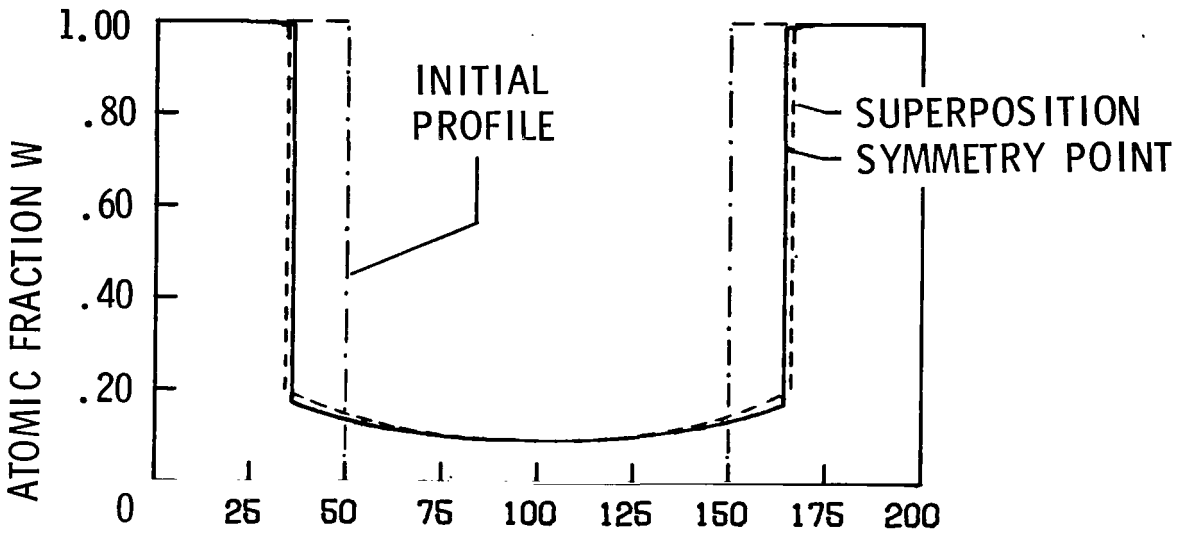

(a) Initial filament volume fraction 0.23.

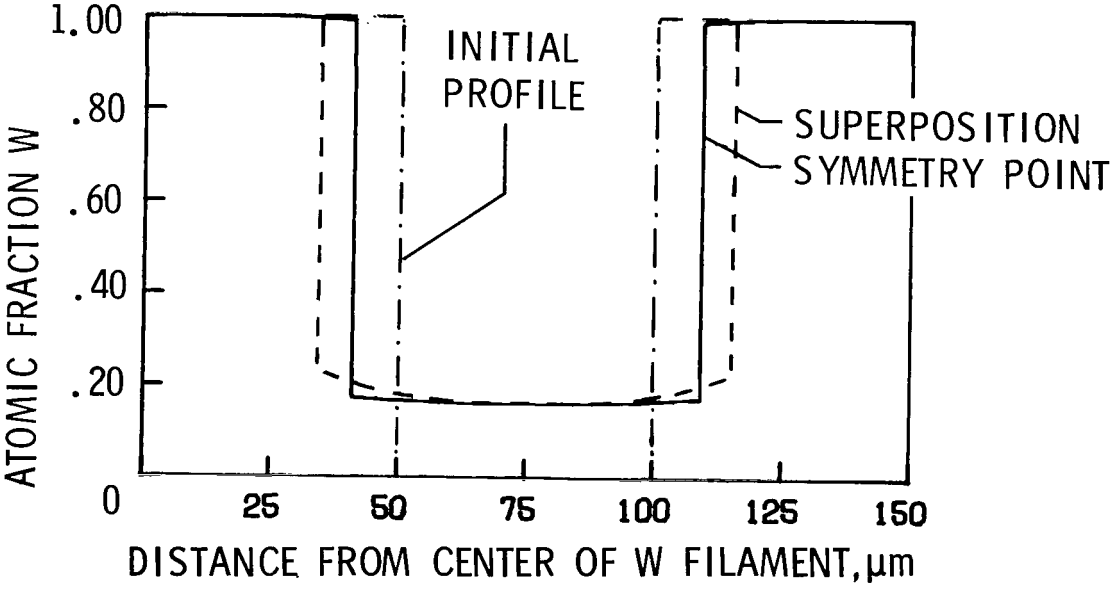

(b) Initial filament volume fraction 0.40.

Figure 7.- Comparison of first nearest neighbor profiles calculated by superposition and symmetry point analysis for W-Ni composites exposed at 1418 K for 500 hours.

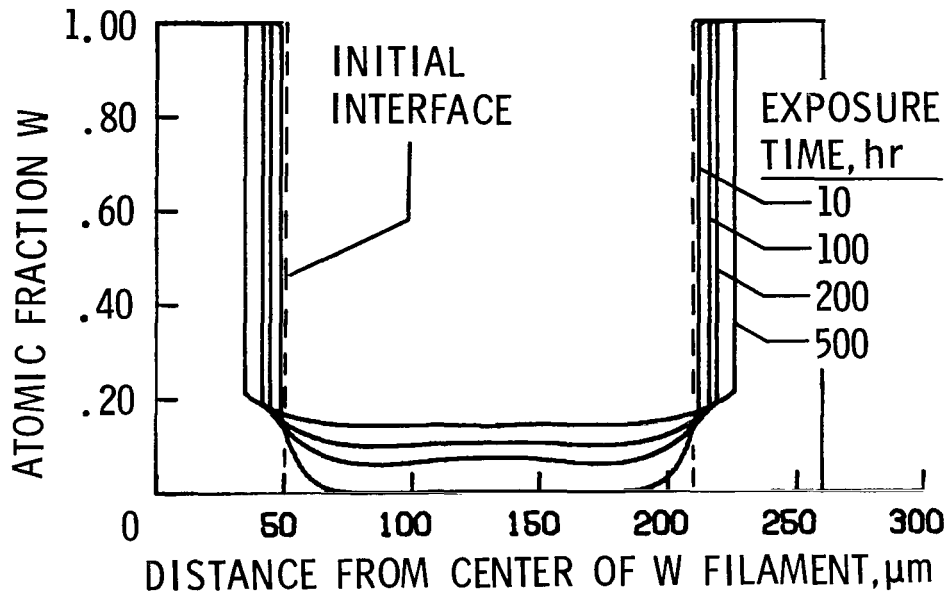

Figure 8.- Concentration profiles between second nearest neighbor filaments calculated by superposition for W-Ni composite $\left(V_f^o = 0.40\right)$ exposed at 1418 K.

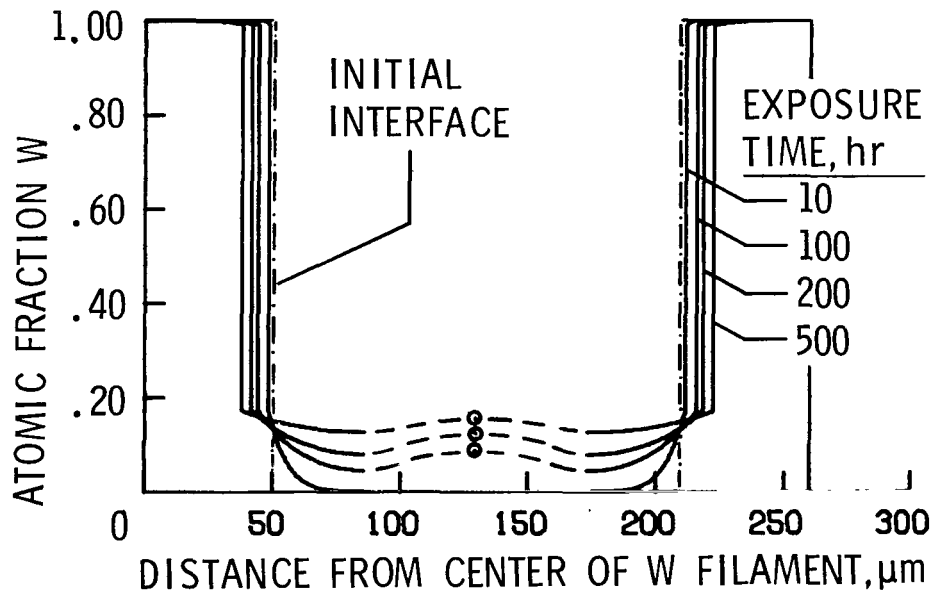

Figure 9.- Concentration profiles between second nearest neighbor filaments calculated by symmetry point analysis for W-Ni composite $\left(V_f^o = 0.40\right)$ exposed at 1418 K.

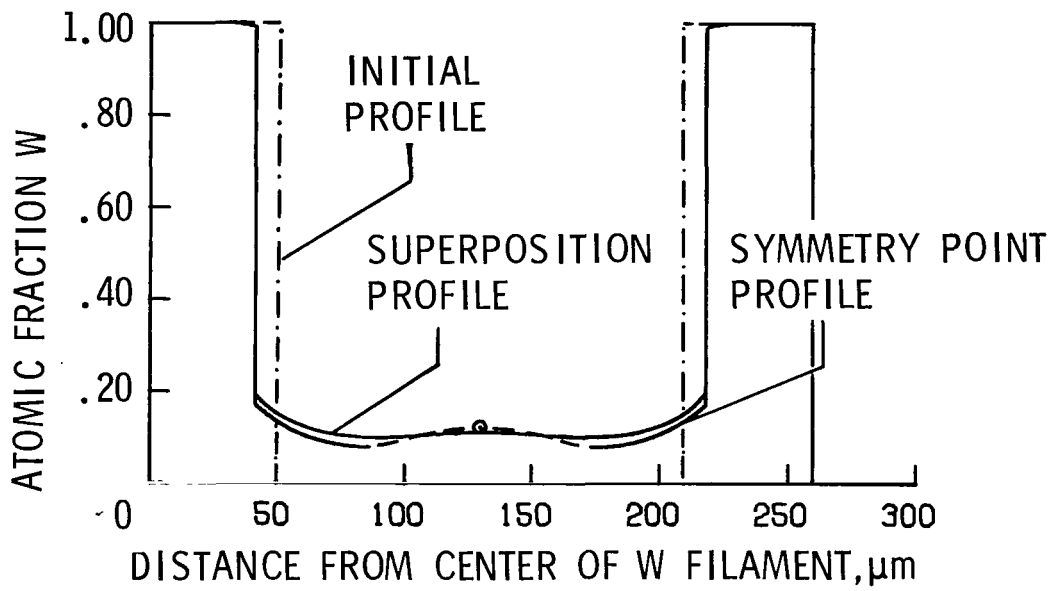

Figure 10.- Comparison of second nearest neighbor profiles calculated by superposition and symmetry point analysis for W-Ni composite $\left(V_{f_.}^{o} = 0.40\right)$ exposed at 1418 K for 200 hours.

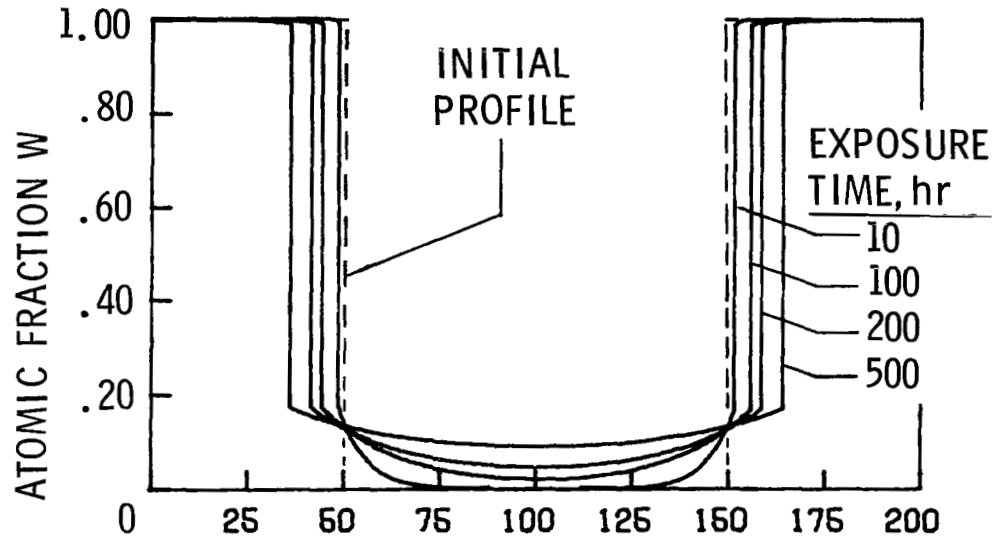

(a) Initial filament volume fraction 0.23.

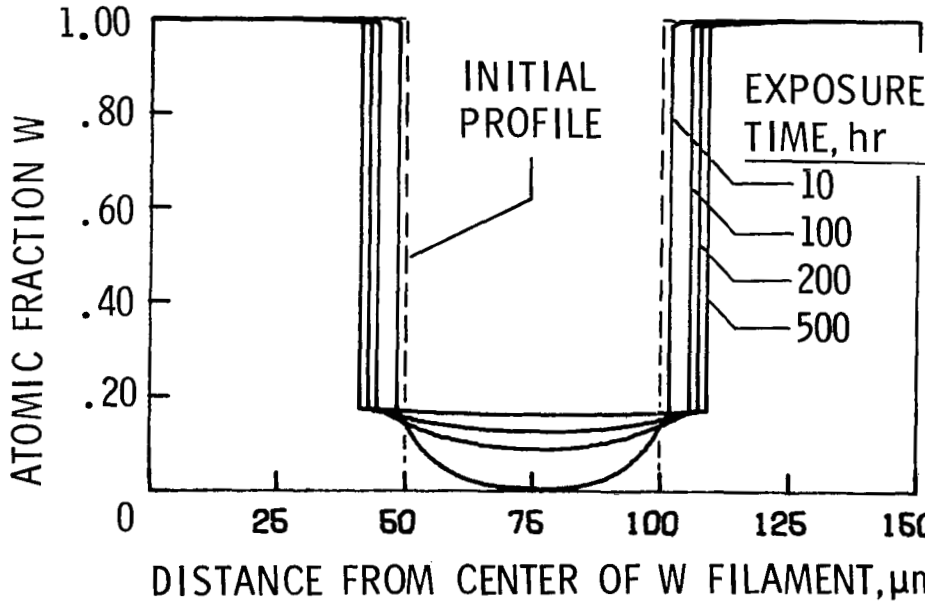

(b) Initial filament volume fraction 0.40.

Figure 11.- Concentration profiles between first nearest neighbor filaments for W-Ni composites exposed at 1418 K.

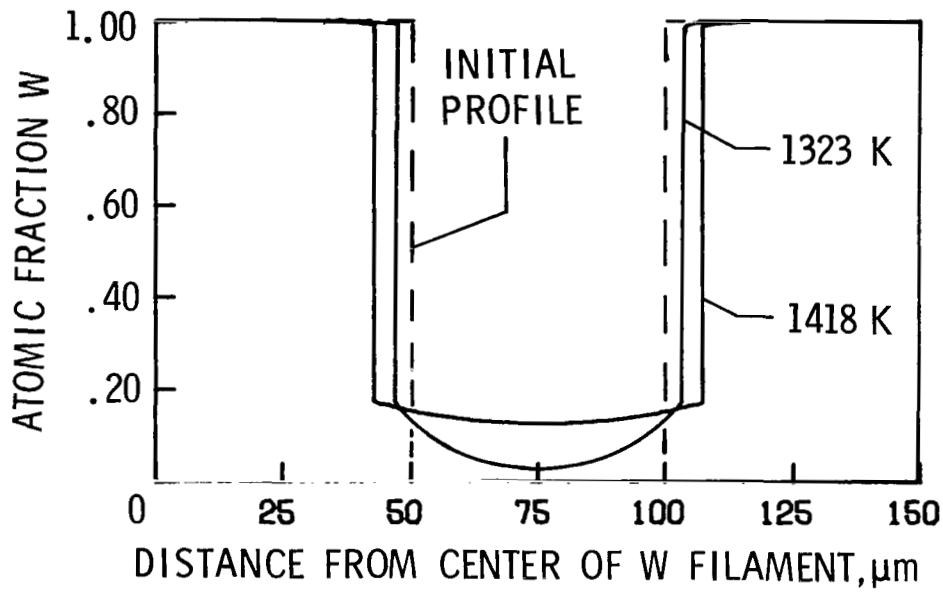

Figure 12.- Comparison of concentration profiles between first nearest neighbor filaments for W-Ni composite $\left(V_f^o = 0.40\right)$ exposed at 1323 K and 1418 K for 200 hours.

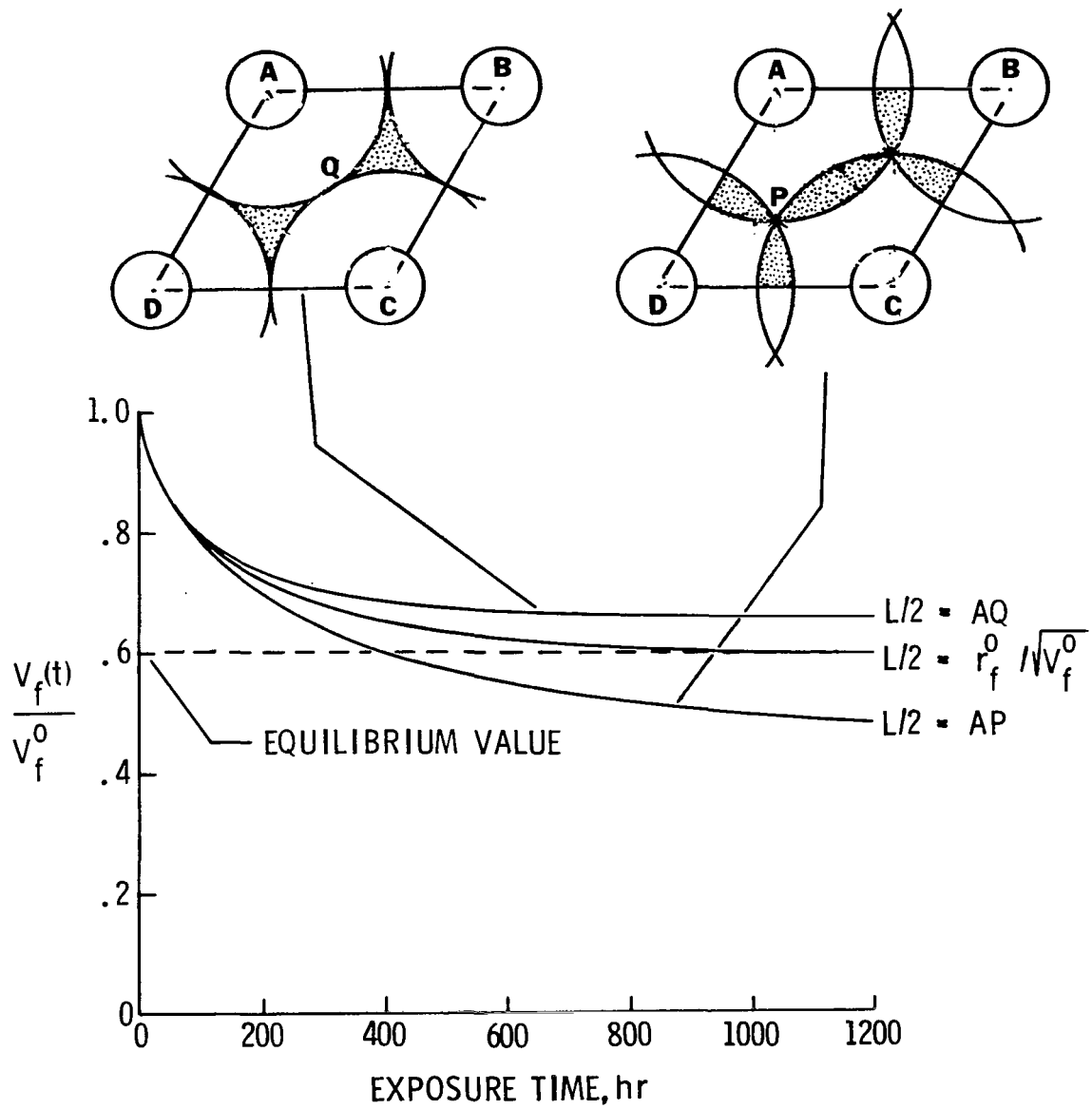

Figure 13.- Comparison of volume fraction decrease curves for three different diameter matrix regions surrounding same size filament in W-Ni composite $\left(V_f^o = 0.40\right)$ exposed at 1418 K.

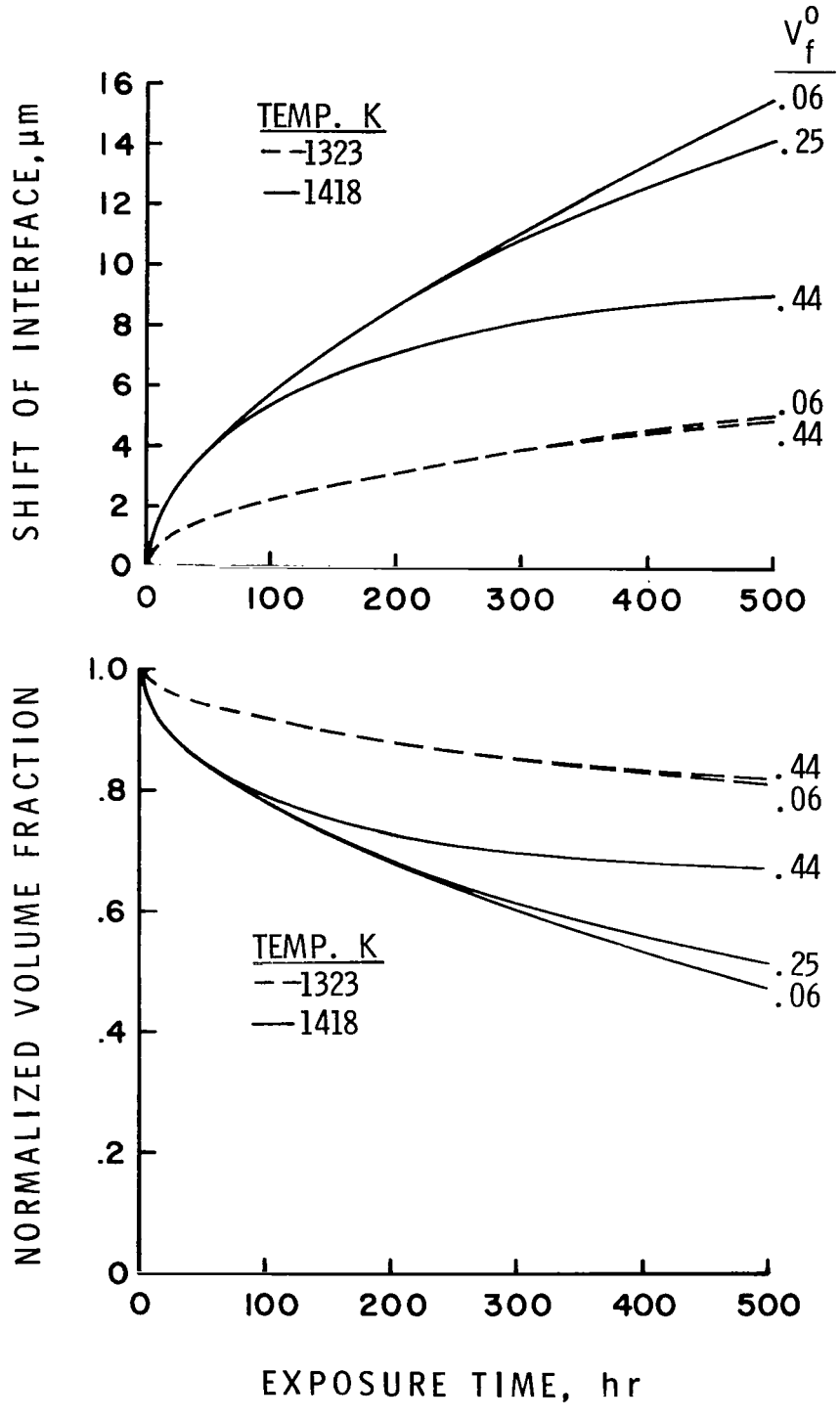

Figure 14.- Shift of W-Ni interface and change in filament volume fraction with exposure time at 1323 K and 1418 K for r_f^o = 50 μm.

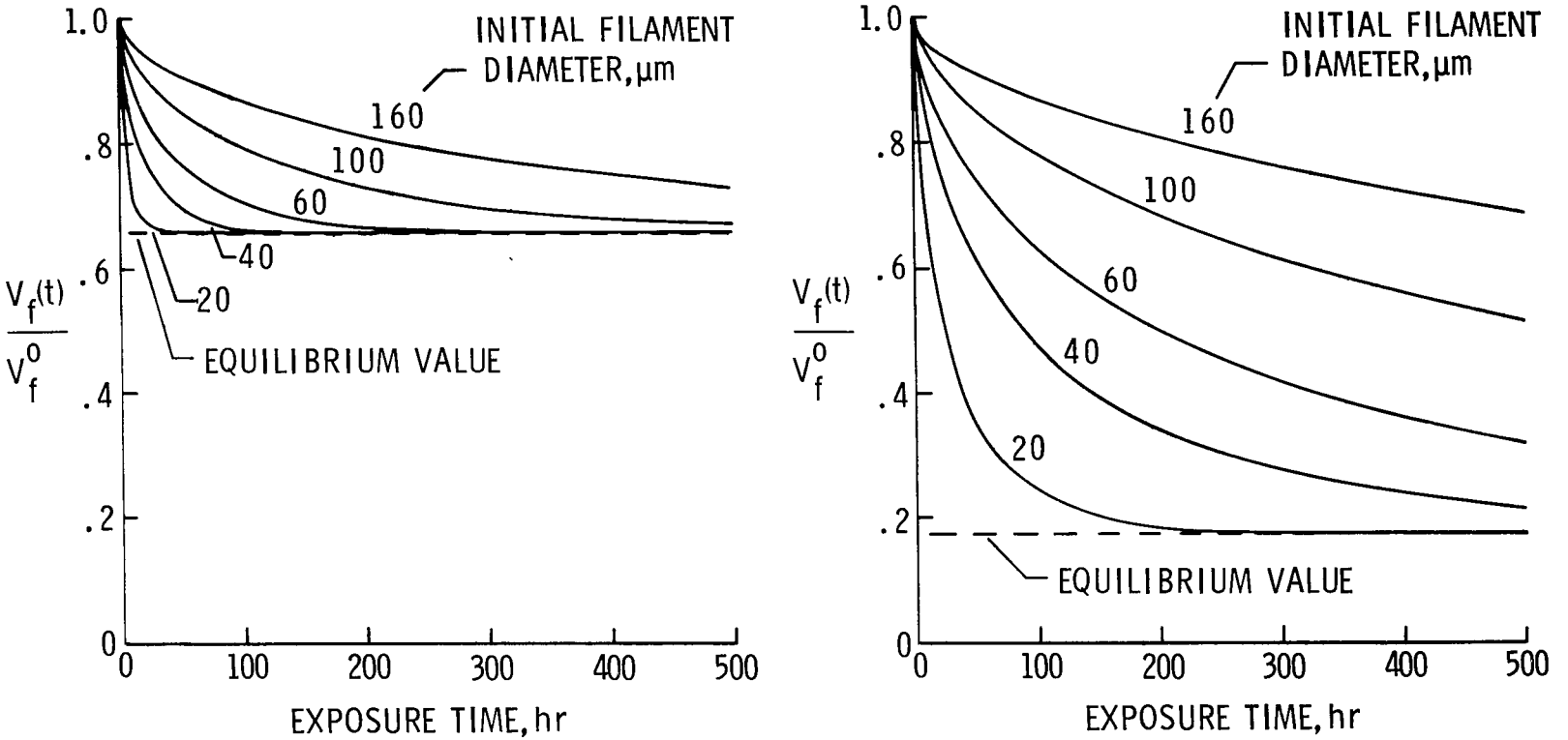

(a) Initial filament volume fraction 0.44.

(b) Initial filament volume fraction 0.25.

Figure 15.- Decrease in normalized filament volume fraction with exposure time at 1418 K for W-Ni composites containing different diameter filaments.

"The aeronautical and space activities of the United States shall be conducted so as to contribute . . . to the expansion of human knowledge of phenomena in the atmosphere and space. The Administration shall provide for the widest practicable and appropriate dissemination of information concerning its activities and the results thereof."

—NATIONAL AERONAUTICS AND SPACE ACT OF 1958

NASA SCIENTIFIC AND TECHNICAL PUBLICATIONS

TECHNICAL REPORTS: Scientific and technical information considered important, complete, and a lasting contribution to existing knowledge.

TECHNICAL NOTES: Information less broad in scope but nevertheless of importance as a contribution to existing knowledge.

TECHNICAL MEMORANDUMS: Information receiving limited distribution because of preliminary data, security classification, or other reasons. Also includes conference proceedings with either limited or unlimited distribution.

CONTRACTOR REPORTS: Scientific and technical information generated under a NASA contract or grant and considered an important contribution to existing knowledge.

TECHNICAL TRANSLATIONS: Information published in a foreign language considered to merit NASA distribution in English.

SPECIAL PUBLICATIONS: Information derived from or of value to NASA activities. Publications include final reports of major projects, monographs, data compilations, handbooks, sourcebooks, and special bibliographies.

TECHNOLOGY UTILIZATION PUBLICATIONS: Information on technology used by NASA that may be of particular interest in commercial and other non-aerospace applications. Publications include Tech Briefs, Technology Utilization Reports and Technology Surveys.

Details on the availability of these publications may be obtained from:

SCIENTIFIC AND TECHNICAL INFORMATION OFFICE

NATIONAL AERONAUTICS AND SPACE ADMINISTRATION

Washington, D.C. 20546